LARGE EDDY SIMULATION OF FINE PARTICLE DEPOSITION IN THERMALLY STRATIFIED TURBULENT CHANNEL FLOW

Yu-Hong Dong* Yimin Tang Lin-Feng Chen

Shanghai Institute of Applied Mathematics and Mechanics,
Shanghai Key Laboratory of Mechanics in Energy Engineering,
Shanghai University, Shanghai 200072, China
*dongyh@staff.shu.edu.cn

ABSTRACT

The dispersion and thermophoresis sedimentation of small inertial particles in a stably stratified turbulent channel flow are studied by means of large eddy simulation. The Lagrangian tracking approach is used to describe the dynamics of particles. Numerical results show that the thermophoresis strengthens the deposition of particles near the cold wall while it weakens the deposition near the hot wall. With the Richardson number increases, the particle mean velocity increases regularly in the core of the channel, and the particle fluctuations intensities decrease under the effect of the buoyancy flux. The magnitude of the thermophoretic forces on particles decreases in the stable thermally stratified flow, which results in smaller deposition rate with increasing the Richardson number.

INTRODUCTION

Transfer and deposition of small inertial particles in turbulent flows is a general phenomenon in environmental, industrial, and biomedical applications (Squires and Eaton, 1991). As one of kind of carried phase, bounded turbulent flows displaying thermal stratification are often present, which are driven by both shear and buoyancy forces (Riley and Lelong, 2000). The buoyancy force has a significant influence on the turbulent transport and internal energy conversion since the velocity and temperature fields are coupled and affected each other. The important processes of bursting, ejection and sweep, consisting of strong vertical motions, are remarkably affected by the stratification effect (Dong, et al., 2004). It's reasonable to predict that the tendency of re-laminarization and weakening of coherent structures of the turbulent flow due to the stable stratification may result in different preferential concentration of particles. Meantime, combining with velocity fluctuations, temperature gradients and thermal stratification, the transport of small particles behaves a complex phenomenon that involves a variety of factors, including coupled interactions between turbulence structures and dispersed phase.

In the thermally stratified flow, the local high temperature gradient in the surrounding fluid may lead to particle thermophoresis and concentration evolution, asides from the influence of the stratification on the particle motion. Thakurta et al. (1998) presented the deposition of small particles under the effect of the thermophoresis. They revealed that the deposition rates of the particle with $\tau^+ = O(1)$ increase dramatically. Zahmatkesh (2008) studied thermophoresis and Brownian diffusion for the deposition of micro- and nanoparticles.

Due to the significance of such problems in environment and engineering, particle-laden flows have been extensively investigated in experiments and numerical simulations in the past few decades. Recently, van Aartrijk and Clercx (2008) reported on light and heavy inertial particles dispersion in forced isotropic and stationary stably stratified turbulence. However, not that many numerical and experimental studies have been devoted to examine the motion of the fine particles in wall-bounded turbulent flows with thermal stratification conditions. Therefore, the influence of both stratification and thermophoresis on the particle transfer across wall-bounded flows should be taken into account more.

In this paper we study fine particle transfer and thermophoretic deposition in the wall-normal direction of a turbulent channel flow under thermal stratification using large eddy simulation and simultaneous Lagrangian tracking. The objective of this study is to examine the influences of thermal stratification and the thermophoresis on the preferential concentration and deposition of small particles with different particle relaxation time scales. The Eulerian approach is adopted for the velocities and temperature field, and spherical particles are simulated in a Lagrangian framework. The dynamic model is applied to predict the effect of subgrid scales in the flow field and the temperature field. The particulate flows are investigated by solving the three-dimensional Navier-Stokes and heat transfer equations under the Boussinesq approximation by use of a fractional-step method coupled with the high-order accurate schemes. The trajectories of particles are calculated by integrating the particle equation of motion consisting of the Stokes drag force, Saffman lift force and thermophoretic force.

MATHEMATICAL FORMULATIONS

1. Particle Equation of Motion

Lagrangian tracking method is used to reproduce the physical situation of particles entrained by a turbulent flow. Here, each case has 100,000 particles tracked in the turbulent flow field with different stratification conditions. The trajectories of a large ensemble of particles are required in

order to present statistics for the dispersed phase in the same manner as for the fluid, i.e., by averaging over homogeneous planes.

The particle equation of motion used here describes the motion of particles with densities substantially larger than that of the fluid and diameters small compared to the Kolmogorov scale ($d_p < \eta$, η the Kolmogrov length scale). Thus the equation includes the Stokes drag force, the Saffman lift force and the thermophoretic force. For particles much heavier than the carrier phase, the influence of virtual mass, the Magnus effect, and the Basset history force on particle motion has been neglected here, their contribution being orders of magnitude smaller than that of the effects considered. Furthermore, Brownian random force has a negligible effect on the particle deposition due to large particle relaxation time here ($\tau_p^+ \geq 1$). The equation is described as follow:

$$\frac{dv_i}{dt} = -\frac{\rho_f}{\rho_p}\frac{3}{4}\frac{C_D}{d_p}|\mathbf{v}-\overline{\mathbf{u}}|(v_i-\overline{u}_i)+f_{li}+f_{Ti}\,. \qquad (1)$$

The first term on the right-hand side of Eq. (6) represents the Stokes drag force. Where d_P is the particle diameter, v_i the particle velocity, and $\overline{u}_i$ the resolved local fluid velocity at the particle position. ρ_f and ρ_p are the fluid and particle mass density, respectively. In this term, the expression for the nonlinear drag correction factor is:

$$C_D = \frac{24}{Re_p}(1+0.15Re_p^{0.687})\,, \qquad (2)$$

where $Re_p = |\mathbf{v}-\overline{\mathbf{u}}|d_p/\nu$ is defined as particle Reynol ds number. The second term f_{li} represents the Saffman lift force (Saffman, 1965). The third term is the thermophoretic force f_{Ti} which acts on the particle due to temperature gradient in the field.

The particle position can be obtained by solving the following relation formula

$$\frac{dx_i}{dt} = v_i\,. \qquad (3)$$

The velocity and trajectory of each particle are simultaneously computed with the carrier phase equations, by means of Lagrangian particle tracking coupled with large eddy simulation. Eq. (2) and (3) are advanced in time by a second-order Adams-Bashforth method. Fourth-order Lagrangian polynomials are used to interpolate the fluid velocities at particle position in Eq. (2). Initially, the particles are set at random locations throughout the channel and their velocities equals to the local fluid velocity. It is assumed that the channel walls are smooth and particles impinging the wall are a fully elastic collision. Particles that exit the domain in the streamwise or spanwise directions are reintroduced into the flow to match the periodic boundary conditions.

2. Simulation of the stratified turbulent flow

In the study, the turbulent flow with thermally stratified condition between plane channels is driven by uniform pressure gradient. The governing equations are the three-dimensional Navier-Stokes equations and the heat transfer equations under Boussinesq approximation. The non-dimensional governing equations by filtering are then given as

$$\frac{\partial \overline{u}_i}{\partial x_i} = 0\,, \qquad (4)$$

$$\frac{\partial \overline{u}_i}{\partial t} + \frac{\partial}{\partial x_j}(\overline{u}_i\overline{u}_j) = -\frac{\partial \overline{p}}{\partial x_i} + \frac{1}{Re_\tau}\frac{\partial^2 \overline{u}_i}{\partial x_j \partial x_j} - \frac{\partial \tau_{ij}}{\partial x_j} + Ri_\tau \tilde{T}\delta_{i2}\,, \qquad (5)$$

$$\frac{\partial \overline{T}}{\partial t} + \frac{\partial \overline{T}\overline{u}_j}{\partial x_j} = \frac{1}{Re_\tau Pr}\frac{\partial^2 \overline{T}}{\partial x_j \partial x_j} - \frac{\partial q_j}{\partial x_j}\,. \qquad (6)$$

Where the overbar denotes application of the filtering operation, $\overline{u}_i$ (i =1,2,3) represents the resolved velocity components in the streamwise (x), wall-normal (y) and spanwise(z) directions, respectively. $\overline{p}$ is the resolved pressure. $Re_\tau = u_\tau \delta/\nu$ represents the Reynolds number and Ri_τ is the Richardson number defined as $Ri_\tau = \beta g \Delta T \delta / u_\tau^2$. ΔT is the temperature difference between the bottom wall and on the top wall. $Pr = \nu/\alpha$ is the molecular Prandtl number with ν the kinematic viscosity of the fluid and α the thermal diffusivity.

In Eqs. (5) and (6), the SGS turbulent stress and heat flux are modeled by the dynamic SGS models (Germano et al. 1994).

$$\tau_{ij} = -2C_\Delta \overline{\Delta}^2 |\overline{S}|\overline{S}_{ij}\,, \qquad (7)$$

$$q_j = -\frac{C_\Delta \overline{\Delta}^2}{Pr_T}|\overline{S}|\frac{\partial \overline{T}}{\partial x_j}\,, \qquad (8)$$

where $\overline{S}_{ij}$ is the resolved rate of strain tensor. Pr_T is the turbulent Prandtl number. The model coefficients C_Δ and Pr_T are dynamically adjusted to the local structure of the flow by the introduction of a test filter with a filter width $\hat{\overline{\Delta}}$ (Wang et al. 2004).

For fully-developed channel flow, periodic boundary conditions for the dependent variables are applied in the streamwise and spanwise directions, and the no-slip and no-penetration velocity conditions are imposed on the walls. Two different constant temperatures, with the top dimensionless temperature being greater than the bottom, are imposed on the bottom and top walls. $T = 0.5$, at the upper wall, $T = -0.5$, at the lower wall. The initial temperature field is set to be a linear distribution along the vertical direction and homogeneous in the horizontal planes.

To validate the present calculation procedure, some typical DNS results for stably and unstably stratified turbulent channel flow performed by Iida et al. (2002) are used to compare with our results. Here, two typical cases for $\mathrm{Re}_\tau = 150$ and $\mathrm{Ri}_b = 0$ and 0.18 (or $\mathrm{Ri}_\tau = 0$ and 12

approximately), where Ri_b is the Richardson number based on the bulk velocity of the turbulent channel flow, are employed to validate the present calculation. Fig.1 shows the distributions of turbulent intensities normalized by the friction velocity and the temperature fluctuation normalized by the friction temperature. It is seen that our calculated results are in good agreement with the DNS data.

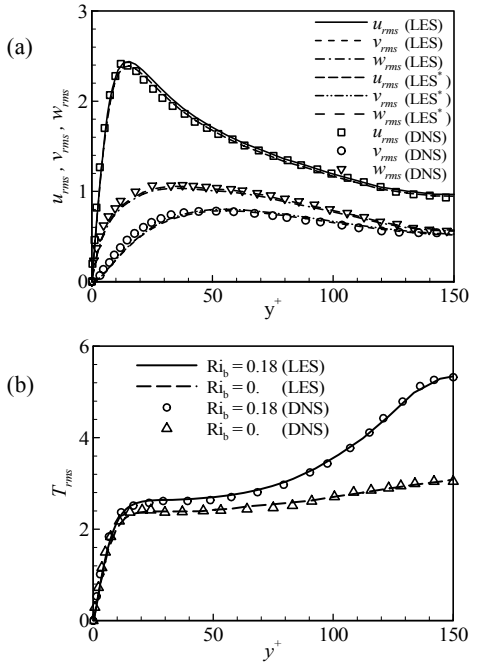

Fig.1. Comparison of the present LES results with DNS data for the turbulent intensities (a) and temperature fluctuation (b).

RESULTS AND DISCUSSION

Some Physical properties of the fluid and particles are given in Table 1. The Reynolds number Re_τ and the molecular Prandtl number *Pr* are set 180 and 0.71 respectively.

Table 1. Physical properties of the fluid and particles

k_p	k_f	ρ_f	λ	ρ_p	T_c
W(m^{-1}K^{-1})	W(m^{-1}K^{-1})	kgm^{-3}	m	kgm^{-3}	K
3.0	0.0259	1.25	6.9x10^{-7}	2500	293

Table 2. Parameters of the particles in channel flow

$d(\mu m)$	d/δ	d^+	τ_p	τ^+
1.0	5.00×10^{-4}	0.090	7.71×10^{-5}	0.937
2.5	1.25×10^{-3}	0.225	4.82×10^{-4}	5.858
3.7	1.85×10^{-3}	0.333	1.05×10^{-3}	12.832
5.0	2.50×10^{-3}	0.450	1.93×10^{-3}	23.434

Simulations are performed for different values of Richardson number and particle relaxation time. The Richardson number is used to characterize the buoyancy effect in stratified flows. Ri_τ equals 0, 10, 20, 30, respectively in our calculations. The particle relaxation time $\tau_p^+ = d^+\rho_p/18\rho_f$.

At the first, statistical quantities of different particle types in the unstratified and stratified flow (Ri_τ =0 and 20, respectively) will be discussed. The parameters of particles used in the simulations are shown in Table 2. d^+ and τ^+ are the dimensionless particle diameter and relaxation time, respectively. Both the mean particle velocity and the particle velocity fluctuations are found to become higher near the wall as τ_p^+ increased, as shown in Fig.1a and Fig.1b. As Ri_τ number increases from 0 to 20 for the case of stably stratified turbulent flow, the flow speeds up and the shear increases. This is evidence that the turbulent boundary layer appears the tendency of re-laminarization in stably stratified flows. Although the velocity profile of each case is very close to each other. It is clear that the mean particles velocities all exceed the fluid velocity at the core region of the channel, while the particles speed up slightly in the sublayer as the particle relaxation time τ_p increases. As the particle relaxation time is rather small, the inertia of particles is small correspondingly, and the particles can easily follow the main motions of the fluid.

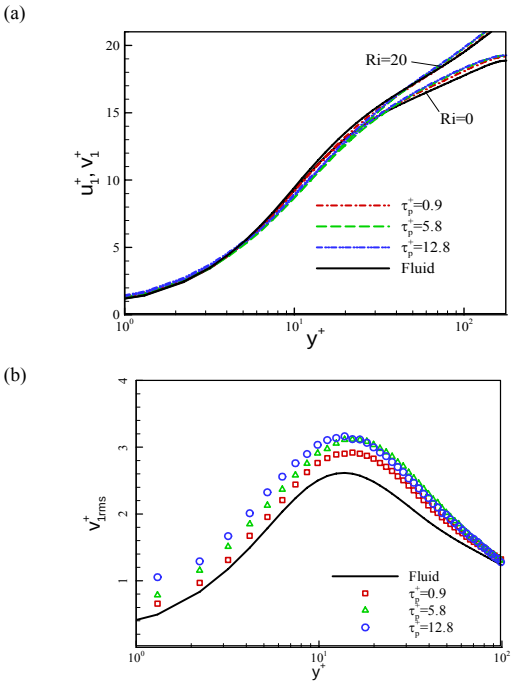

Fig. 1 Mean streamwise fluid and particle velocity profiles (a), rms streamwise velocity fluctuations (b).

We are also investigate the three key forces, i.e. the normal component of the Stokes drag force, the lift force and

the thermophoretic force acting on the particles for different particle relaxation time for Ri_τ=20. Fig. 2 shows the relative contributions of the different forces on the particle deposition.

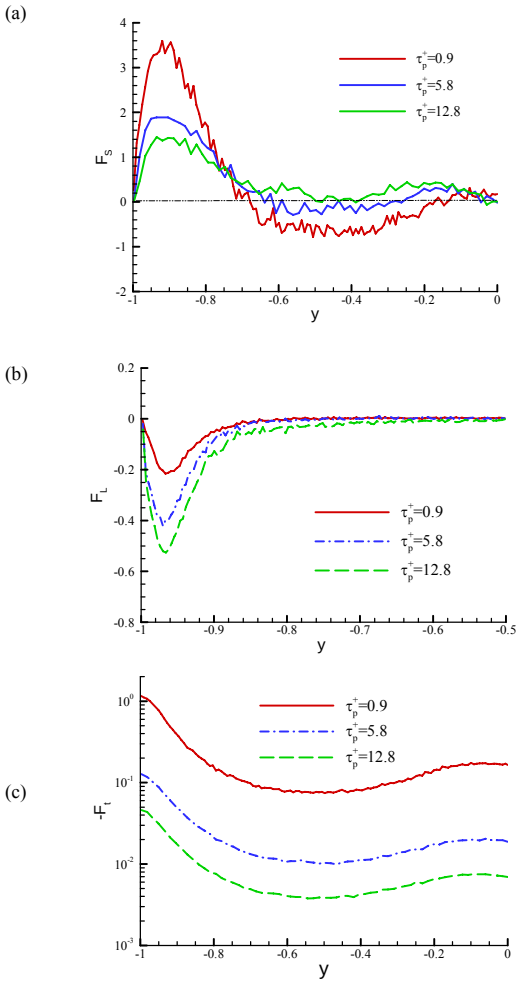

Fig.2 Comparison of the averaged magnitude of the normal component of each force. (a) the Stokes drag force; (b) the Saffman lift force; (c) the thermophoretic force..

Even if the normal component of Stokes drag force plays most important role on determining particle dynamics when $\rho_p >> \rho_f$ comparing the other forces, Saffman lift due to velocity gradient and thermohophoresis due to temperature gradient become non-negligible within the viscous sublayer.It is apparent that the magnitude of the force decreases with the increasing particle relaxation time. Fig. 2b and 2c show the average lift force and the thermophoretic force acting on the particles, respectively. It is apparent that the magnitude of the force decreases with the increasing particle relaxation time. From the peak of the profiles of the forces, we may find why the particles travel rapidly toward the wall. Fig. 2b and 2c show the average lift force and the thermophoretic force acting on the particles, respectively. It can be noticed that the lift force is significant only in the viscous sublayer for -1<y<-0.9 (y^+ <20) as shown in Fig. 2b, and then it diminishes rapidly in the core of the channel. We may find the fact that the thermophoretic force plays a necessary role in deposition for smaller particles as shown in Fig. 2(c). Here, the thermophoretic force decreases rapidly as the particle diameter increases. The magnitude of the thermophoretic force acting on the particle relaxation time 0.9 is approximately 10 times larger than that acting on particle particle relaxation time 12.8 under the same conditions. As may be observed, that for increasing the particle relaxation time the thermophoretic force is reduced.

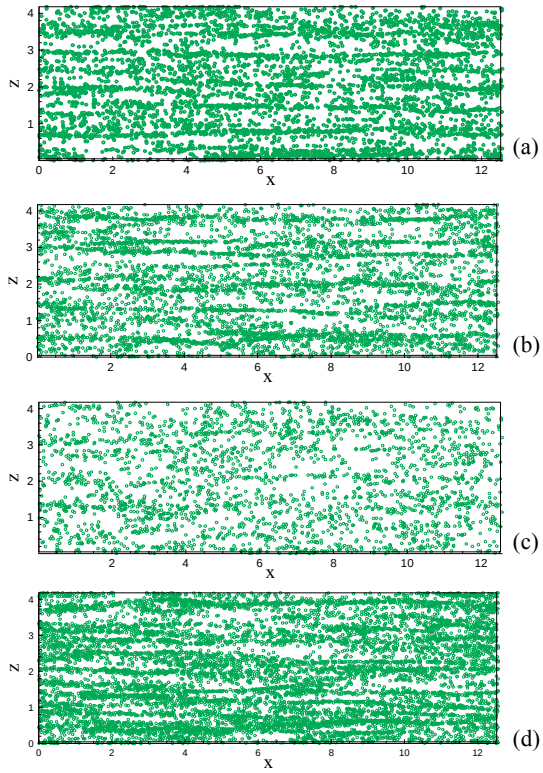

Fig. 3. Particle distributions in the viscous sublayer. (a) and (b) without thermophoresis; (c) and (d) with thermophoresis. (a) and (c) near the hot wall (1.3<y^+<8.6); (b) and (d) near the cold wall (1.3<y^+<8.6).

Fig. 3 shows the instantaneous number density distributions at the same plane near the both walls. It is seen that the particles preferentially concentrated along narrow regions which correspond to the low-speed regions in the Fig. 3a and 3b, when the influence of the thermophoretic force is not considered. However, there is a remarkable difference for the particle distributions between the cases for which the thermophoretic force is presented or not. Fig. 3c and 3d show the instantaneous particle distribution with the condition which temperature gradient is imposed in the channel, particularly, high temperature gradient occurs in the viscous

sublayer. We examine then the influence of both the particle relaxation time and the thermal stratification on particle deposition rate. Fig. 4 shows the particle deposition rate versus the particle relaxation time obtained for Ri_τ=0 and 20, comparing with some simulational results and experimental observation. As far as we concerned range of τ^+, the deposition rate without thermophoresis increases quadratically with particle relaxation time which is in agreement with that obtained from the experimental data (McLaughlin, 1989). It can be seen that, when the thermophoretic force is included, the computed deposition rate is consistently higher than the value without thermophoretic force.

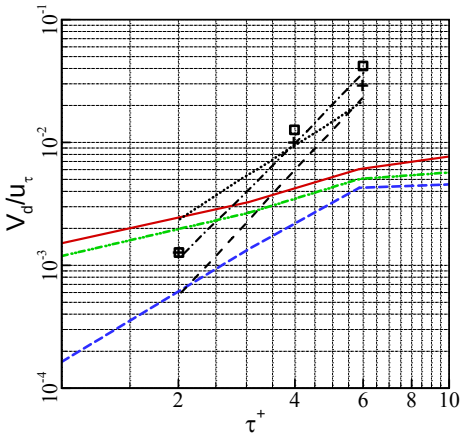

Fig. 4. Particle deposition rate near the cold wall.... Liu & Agarwal (1974); McLaughlin (1989): □ $\rho = 713$, + $\rho = 1500$; Wang & Squires (1996): -·- ρ =713, - - - $\rho = 1500$; Present: ρ =2000, – – without thermophoresis, — with thermophoresis (*Ri*=0), -·-·- with thermophoresis (*Ri*=20).

CONCLUDING REMARKERS

We studied transfer and deposition of small inertial particles in a thermally stratified turbulent channel flow using large eddy simulation and Lagrangian particle tracking. The key issues are the influence of stratifications，the particle relaxation time, and thermophoresis on the particle dynamics. The motion of particles in the stratified turbulent flow is determined by Stokes drag force, as well as Saffman lift，the thermophoretic force due to the inhomogeneous distribution of the hydrodynamic and temperature fields. The particle concentrations in the sublayer increased with increasing the particle relaxation time. The thermophoresis strengthens the deposition of particles near the cold wall while it weakens the deposition near the hot wall. Comparing the concentration and deposition rate between with and without thermophoresis, it is clear that the thermophoresis under the positive temperature gradient raised remarkably the deposition of particles. With the Richardson number increases, the particle mean velocity increased regularly in the core of the channel. And the particle rms fluctuations in the stratified flow lagged below that in the unstratified flow. The magnitude of the thermophoretic forces of particles decreases in the stratified flow, which resulted in the deposition of particles near wall region reduces with increasing the Richardson numbers.

ACKNOWLEDGEMENTS

This work was supported by the NSFC (10972132), the Shanghai Municipality Education Committee (09YZ03), and the Shanghai Sci. & Tech. Committee (08JC1409800).

REFERENCES

Squires K. D., Eaton J. K., 1991. Preferential concentration of particles by turbulence, *Phys. Fluid A* 3, 1169-1178.

Riley, J. J., Lelong, M. P., 2000. Fluid motions in the presence of strong stable stratification. *Annu. Rev. Fluid Mech*. 32, 613–657.

Dong Y. H, Lu X. Y., Zhuang L. X., 2004 Large eddy simulation of a thermally stratified turbulent channel flow with temperature oscillation on the wall, *Int. J. Heat Mass Transfer*, 47, 2109-2122.

Thakurta D. G., Chen M., McLaughlin J. B., Kontomaris K., 1998. Thermophoretic deposition of small particles in a direct numerical simulation of turbulent channel flow. *Int. J. Heat Fluid Flow* 41, 4167-4182.

Zahmatkesh I., 2008. On the importance of thermophoresis and Brownian diffusion for the deposition of micro- and nanoparticles. *Int. Communications Heat Mass Transfer* 35, 369-375.

van Aartrijk M., Clercx H. J. H., 2008. Preferential concentration of heavy particles in stably stratified turbulence. *Phys. Rev. Lett.* 100, 254501.

Saffman, P. G., 1965. The lift on a small sphere in a slow shear flow. *J. Fluid Mech*. 22, 385-340

Germano M., Piomelli U., Moin P., Cabot W., 1991. A dynamic subgrid-scale eddy viscosity model. Phys. Fluids 3, 1760-1765.

Wang L., Dong Y. H., Lu X. Y., 2005，An investigation of turbulent open channel flow with heat transfer by large eddy simulation. Comput. & Fluids 34, 23-47.

Iida O., Kasagi N., Nagano Y.,2002, Direct numerical simulation of turbulent channel flow under stable stratification, *Int. J. Heat Mass Transfer* 45, 1693-1703.

McLaughlin J. B., 1989. Aerosol particle deposition in numerically simulated channel flow. *Phys. Fluids* A 1, 1211-1224.

Wang, Q., Squires, K. D., Wu, X., 1995, Lagrangian statistics in turbulent channel flow, *Atmospheric Environment*, 29,2417-2427.

Liu B. Y. H., Agarwal J. K., 1974. Experimental observation of aerosol deposition in turbulent flow. *AerosolScience*5,145-155.